JOURNAL OF
EMERGING INVESTIGATORS

Article

Photometry of the Type II supernova 2025ngs

Florence Bavas[1*], Abraham Gerstein[2*], Kelly Haberkorn[3*], Milam Garrett[4], Michael Warrener[5], Michael Faison[5]

[1] Martin Luther King Jr. Magnet High School, Nashville, Tennessee
[2] Albuquerque Academy, Albuquerque, New Mexico
[3] Garfield High School, Seattle, Washington
[4] Grand Oaks High School, Spring, Texas
[5] Department of Astronomy, Yale University, New Haven, Connecticut
*These authors contributed equally to this work

SUMMARY

Through observations of supernovae, we can quantify their changes in brightness and therefore better understand astrophysical processes of stellar evolution. This contributes to the study of the formation of heavy elements that occur in a star's core and eventually make up the universe. We selected a recent extragalactic supernova, 2025ngs, and studied its change in magnitude of brightness over time to determine its type and distance from Earth. We chose this supernova because of its relative youth and high discovery brightness. We hypothesized that 2025ngs would be a Type II supernova because of prior reports of hydrogen emission features, identified by the wavelengths of light emitted by the supernova. These specific wavelengths emitted by hydrogen are a defining feature of Type II supernovae. We imaged 2025ngs over three weeks in both the Sloan g and r color bands. We then performed differential photometry to obtain its standard apparent magnitude across the observation time frame. We produced a light curve and compared it to model light curves with least-squares fitting to determine the type of supernova. We found 2025ngs to be a Type II-P supernova, with a characteristic peak at a standard apparent g magnitude of 17.258 followed by a plateau at g 17.874 for ≥ 7 days, which is consistent with the typical shape of Type II-P light curves. These results contribute to a broader understanding of Type II-P supernovae. Collecting more data on these light curves allows the astronomical community to home in on the exact aspects that differentiate these plateauing supernovae from the others.

INTRODUCTION

As massive stars reach the end of their evolutionary cycle, they eventually cannot support their own mass and explode, becoming supernovae. The study of supernovae is particularly helpful in understanding the chemical composition of celestial objects, the interstellar medium, stellar evolution, and the expansion of the universe. Supernovae either result from a massive star's core collapsing, or from a white dwarf accumulating matter exceeding its upper limit (1).

Supernovae can be classified by looking at their spectrum of wavelengths emitted or with the supernova's light curve: a graph of the supernova's magnitude (or brightness) over time. Classifying the different types of supernovae is an important aspect of understanding our universe, as Type Ia supernovae serve as distance markers because of their standard luminosity and all supernovae differentiate diverse star life cycles that reveal more about the functions and processes of stars across the universe (1).

Type I supernovae are categorized by a lack of hydrogen and are further subcategorized by cause (core collapse or white dwarf). Type Ia supernovae occur in binary star systems, which consist of a white dwarf star and another star orbiting each other. The white dwarf accumulates mass from the other star until it reaches its mass limit, designated as the Chandrasekhar mass. (2). Once the white dwarf reaches this mass, it explodes from excessive pressure (1). Type Ib supernovae are the result of a massive star's core collapsing in on itself (1). After the collapse, the star expands again, pushing off its hydrogen layer (1). Similarly, Type Ic supernovae are the result of core collapse of a massive star, but these supernovae expel both their hydrogen and helium layers (1). Type 1a light curves show a steep increase in magnitude followed by a steady decline, while Type Ib light curves have a steadier increase followed by a relatively slow decrease in magnitude (1). Type 1c light curves are categorized by a steep decrease in magnitude, followed by a steady, slower decrease (1).

Type II supernovae all result from core collapse, like Type Ib and Ic, but they contain hydrogen. The two most prominent Type II supernovae subtypes are linear (SNII-L) and plateau (SNII-P) (3). After SNII-L reach peak magnitude, their apparent brightness rapidly decays, while SNII-P will maintain a constant brightness for an extended period of time, creating the plateau of their light curves (3). Conversely in SNII-Ps, as the stellar ejecta, or the matter being expelled, expands, the plateau phase is caused by a change in opacity of the outer layer of the star (3). The shock wave from the core ionizes hydrogen, thus making it more opaque and preventing radiation from escaping as it would in an SNII-L (3). Hydrogen then recombines at a fixed temperature in what is called the photosphere (3). As the ejecta expands and cools, the photosphere recedes inwards to maintain a constant temperature and therefore causes a plateau in brightness (3). While not as common, there are two other Type II supernovae, which can be distinguished by looking at the elements present in the star's spectral lines. Type IIn supernovae are distinct because their hydrogen layer is ejected before the star explodes, and Type IIb supernovae begin like a Type II supernova, releasing similar amounts of hydrogen, but eventually have helium emissions only, like Type Ib supernovae (4).

Astroid Terrestrial-impact Last Alert System (ATLAS)

https://doi.org/10.59720/26-016

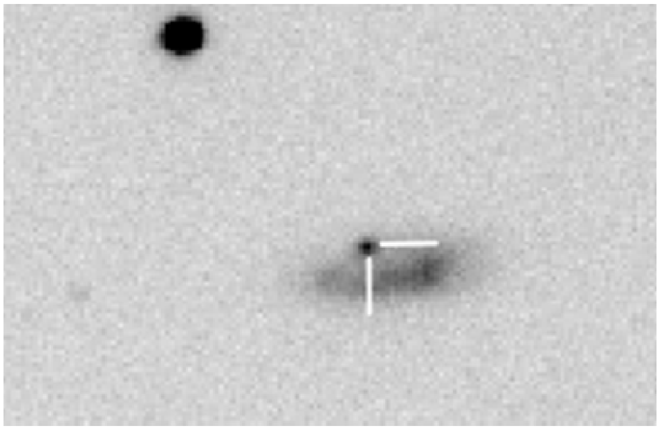

Figure 1. Image of supernova 2025ngs, indicated by white markers, in galaxy NGC 5961. Taken on T11 telescope from the Remote Desert Observatory through itelescope.net on July 8th, 2025.

discovered supernova 2025ngs in the spiral galaxy NGC 5961 on June 6th, 2025, at a right ascension of 15h35m16.678s and a declination of +30°51'55.67" (5). Prior research on this supernova had identified its helium and hydrogen emission lines, based on the specific wavelengths that these elements emit (6). This led us to hypothesize 2025ngs was a Type II supernova. 2025ngs did not have any previously published light curves, so we could not hypothesize a subtype. Our findings support our hypothesis that 2025ngs **(Figure 1)** is a Type II supernova and suggest that it is specifically a SNII-P. Additionally, we determined 2025ngs to be about 35.481 ± 2.276 megaparsecs (Mpc) away from Earth (7). This means 2025ngs is close to 116 million lightyears or one sextillion kilometers away. This research finds and proves the exact supernova type of 2025ngs correspondent with its light curve, contributing to the broader astronomical community's classification of supernova.

RESULTS

We took measurements of the supernova throughout July 2025, observing on clear days and prioritizing times when 2025ngs had the highest altitude to avoid interference from Earth's atmosphere. We used the 0.4-meter telescope at the Leitner Family Observatory and Planetarium and the T11 telescope at the Utah Remote Desert Observatory to obtain seven total measurements of 2025ngs **(Table 1)**.

For each of the seven measurements of 2025ngs, we found standard magnitudes, color indices, and uncertainties. Apart from the Sloan r magnitude measurement from June 17th, 2025, our magnitudes from both filters steadily decreased before reaching a plateau **(Table 2)**. The g-r color index increased over time.

We determined 2025ngs's type by plotting the light curve of our data and fitting it to models of five potential supernova types **(Figure 2).** We performed this model-fitting by calculating the chi-squared value over a grid of y-offset values, x-offset values, and stretch factors. While Type I supernovae, especially Type Ia, tend to have very little variation in their light curves, Type II supernovae vary significantly (8). We chose to use stretch factors for the Type II supernovae models to account for the fact that our models had fixed magnitudes and could not capture this variation. For the Type IIb supernova model, adding a stretch factor did not improve the chi-squared value. Our graph also indicated that if 2025ngs were a Type IIb supernova, we did not make observations early enough to capture the irregularities in its light curve. The most accurate data would show the supernova's magnitude increasing, reaching its peak, decreasing, and then plateauing; however, our data only showed a decrease in magnitude followed by a plateau. Thus, we chose to apply stretch factors to the models for SNII-L and SNII-P.

The light curve for a SNII-P had the lowest chi-squared value, 0.321, and therefore fit best to our data. We used a stretch factor of 1.9. The peak brightness of 2025ngs occurred on July 6th, 2025, two days before our first measurement **(Figure 3)**. On that day, the supernova reached a peak Sloan

Julian Date	*Telescope*	*Exposure Time (s)*	*Airmass*	*Weather*	*Lunar Illumination*
2460865.775	*T11*	*120*	*1.11*	*Clear Skies*	*90.5%*
2460867.775	*T11*	*120*	*1.12*	*Clear Skies*	*100.0%*
2460874.878 a.	*0.4-meter RCT*	*60*	*1.16*	*Clear Skies*	*50.0%*
2460879.587	*0.4-meter RCT*	*60*	*1.06*	*Clear Skies*	*1.7%*
2460882.687	*0.4-meter RCT*	*45*	*1.08*	*Clear Skies*	*0.9%*
2460884.617	*0.4-meter RCT*	*45*	*1.13*	*Cloudy at end of observing*	*9.3%*
2460886.674	*0.4-meter RCT*	*45*	*1.38*	*Clear Skies*	*24.0%*

a. *The dark frames were insufficient and could have affected data validity.*

Table 1. Conditions during the telescopic observation of SN2025ngs. This table includes information about the conditions present when observing SN2025ngs between July 8th – July 29th, 2025, as well as the telescope and exposure time used for each observation. RCT stands for Ritchey-Chrétien Telescope, a specific kind of telescope with two hyperbolic reflecting mirrors

Julian Date	*Sloan g Magnitude*	*g Uncertainty*	*Sloan r Magnitude*	*r Uncertainty*	*g-r Color index*
2460865.775	*17.294*	*0.056*	*16.548*	*0.119*	*0.746*
2460867.775	*17.393*	*0.062*	*16.581*	*0.108*	*0.811*
2460874.878	*17.773*	*0.130*	*16.988*	*0.172*	*0.785*
2460879.587	*17.853*	*0.097*	*16.688*	*0.118*	*1.164*
2460882.687	*17.908*	*0.129*	*16.696*	*0.163*	*1.212*
2460884.617	*17.913*	*0.099*	*16.770*	*0.123*	*1.145*
2460886.674	*17.906*	*0.101*	*16.751*	*0.154*	*1.155*

Table 2. Photometric data for 2025ngs. Observed magnitudes—instrumental magnitudes corrected for atmospheric extinction, instrument sensitivity, and zero points—alongside uncertainties calculated using the root mean square for each observation.

JOURNAL OF
EMERGING INVESTIGATORS

https://doi.org/10.59720/26-016

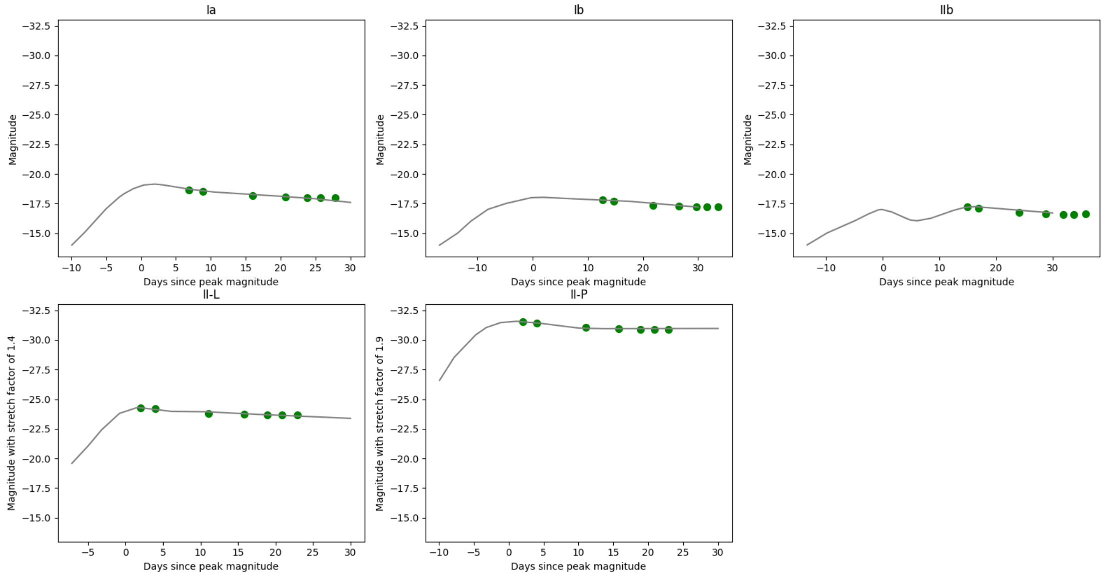

Figure 2. Lowest chi-squared fits for days since peak magnitude versus absolute magnitude for each type of supernova modeled. All data is in the Sloan g filter. Each graph shows the best fit of a given light curve to our data. The magnitudes for Type II-P are stretched with a stretch factor of 1.9. The reduced chi squared values are: 1a = 3.550, Ib = 1.414, IIb = 3.526, II-L = 0.696, and II-P = 0.321.

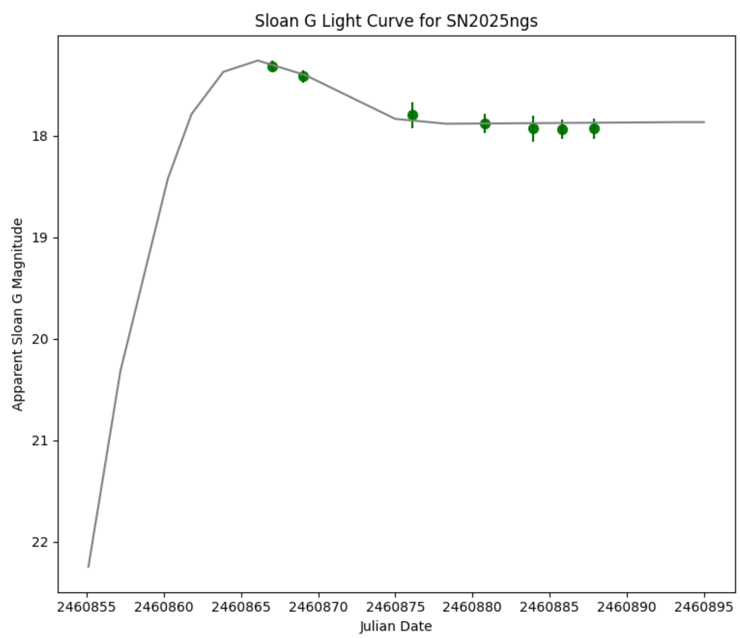

Figure 3. Type II-P light curve for 2025ngs in the Sloan g band. Observed with a reduced chi-squared value of 0.32. The error bars represent the Sloan g uncertainty, calculated by taking the root mean squared of the residuals of each line of best fit.

https://doi.org/10.59720/26-016

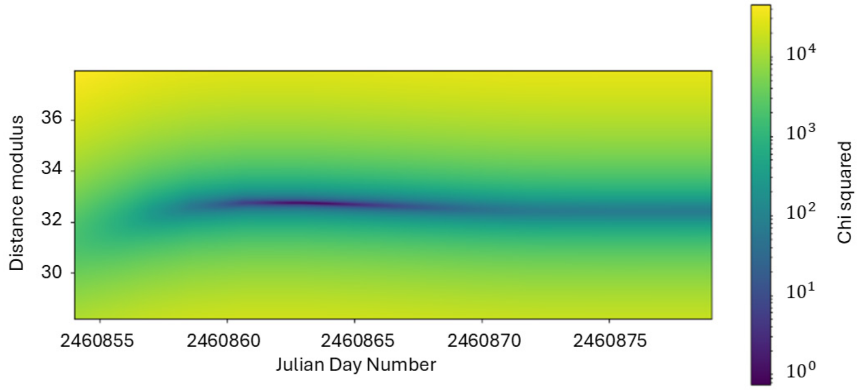

Figure 4. Approximation of distance modulus for supernova 2025ngs. This contour map shows chi-squared values for the Julian Day Number of the supernova's peak magnitude and the distance modulus, representing the distance to the supernova. The lowest chi-squared value occurs at approximately Julian Day 2460863 and distance modulus 32.750 ± 0.135.

g magnitude of approximately 17.258. Using the distance modulus obtained from our data, we determined 2025ngs's distance to be approximately 35.481 ± 2.276 Mpc away **(Figure 4)**.

DISCUSSION

Through aperture photometry and model fitting, we identified 2025ngs as a Type II-P supernova and recorded its magnitude and color over three consecutive weeks. We submitted these data to the American Association of Variable Star Observers (AAVSO) and performed our own analysis. The supernova decreased in magnitude during the entire duration of our observations, meaning that its peak magnitude occurred before we began collecting data. After their peak, Type II-P supernovae decrease in brightness, plateau, and then decrease again (9). Our observations ended less than a week into 2025ngs's plateau at magnitude 17.874. The exact duration of the supernova's plateau depends on the size of the star's hydrogen envelope, but lasts an average of approximately 100 days (3, 10). Since we only observed 2025ngs for about 3 weeks after its predicted peak magnitude and beginning of its plateau, we were unable to see it decrease in magnitude.

SNII-Ps are one of the most common types of supernovae, appearing frequently throughout observable galaxies (11). However, the maximum magnitude of Type II-P supernovae is often fainter than that of other supernova types, making them more difficult to discover and observe (12). The high chance of observing a Type II-P supernova and our reduced chi-squared value of 0.321 provide strong evidence to support our model fitting (13). The light curve for the Type II-L supernova had a low reduced chi-squared value of 0.7 and could be another, less likely, option for classifying 2025ngs. Our chi-squared values, trends in our data, and relative abundance of Type II-P supernovae suggest that a plateau rather than a linear descent is most likely. Additionally, other stretch factors and x offsets of up to 15 days can also produce reduced chi-squared values under 5 using the II-P light curve model. Due to this, 2025ngs may have reached its peak magnitude longer before our first observation than our model suggests. Measurements taken outside of our research group show 2025ngs peaking in late June rather than our measured time of July 6 (5).

It is possible to fit our data in a model for SNII-Ps that would indicate an earlier peak magnitude by applying a very large stretch factor. In the future, we could search for alternative models of Type II-P supernovae that have more variation in their magnitudes to better represent our data. The current model fits our data best and accurately represents the supernova type and magnitude over time, but may have errors in its peak magnitude and the date when the peak magnitude occurred.

Our calculated distance of 35.481 ± 2.276 Mpc also differs statistically from the accepted distance to NGC5961, the supernova's host galaxy, which is at a distance of 31.8 Mpc and does not fall within our uncertainty (14). Our calculated distance may be farther than the accepted distance because we lack precise measurements from our SN2025ngs's peak magnitude. The most common method for calculating distance to Type II-P supernovae is the Expanding Photosphere Method, which is calculated by measuring the angular size and expansion velocity of the supernova's photosphere (15). Since our data did not allow us to calculate these values, we instead used the distance modulus to calculate distance, which compares absolute versus apparent magnitudes.

However, Type II-P supernovae are not standard candles, unlike Type Ia supernovae that have a known absolute magnitude (1). This means our peak magnitude and distance modulus are both approximations. Additionally, various estimates of the distance modulus and the date when the supernova reached peak magnitude produced a reasonable

https://doi.org/10.59720/26-016

chi-squared value when fitting our data to a light curve. If we took more measurements in the future or worked on a similar project, we would aim to gather more data to improve our distance modulus estimate or try the Expanding Photosphere Method for finding the distance.

Our green magnitudes decreased and then plateaued following the light curve, but our red magnitudes decreased at a slower rate, causing an increase in color index over time. The redness of 2025ngs aligns with its status as a Type II-P supernova: the large amounts of hydrogen present surrounding Type II-P supernovae cause red light to be emitted because hydrogen has a strong red emission line (16). Additionally, the color index depends on temperature, becoming larger as a star cools (16). Depending on the supernova, significant changes to the g-r color index can be seen in as little as two weeks. Our measurements of decreasing magnitude and increasing color index indicate the cooling of 2025ngs over time, though some of the change in color index may be due to uncertainty or measurement errors. Specifically, limited calibration stars and the usage of square instead of circular apertures could have reduced the precision of the best-fit lines we used to calculate color. Additionally, 2025ngs is inside host galaxy NGC 5961, which could have interfered with measurements. With more time, our research group may collect more data from 2025ngs, with the aim of obtaining an even more precise estimate of its distance, color, and properties.

Our research contributes to the scientific understanding of Type II-P supernovae, their properties, and stellar evolution. Further research concerning 2025ngs could focus on determining the plateau time, which can be used to make inferences about the mass and energy of the ionized hydrogen surrounding the star. Additionally, broader research could identify other Type II-P supernovae within host galaxies such as ours and compare their magnitudes, colors, and plateau time to 2025ngs, or look for younger Type II-P supernovae to measure magnitudes throughout their whole lifespan.

MATERIALS AND METHODS

Image acquisition

Images of 2025ngs were obtained over three weeks of observation using two different telescopes. Primary observations were conducted with the 0.4-meter f/8.9 telescope at the Leitner Family Observatory and Planetarium at a latitude of 41.3210° N and a longitude of 72.9220° W. Supplementary data were acquired through the remote observation service iTelescope, using the T11 telescope at the Utah Remote Desert Observatory at a latitude of 37.7379° N and a longitude of 113.6975° W (17). This service was used to capture images when local telescope time was not allocated or when 2025ngs was otherwise obscured due to inadequate weather **(Table 1)**.

All data recorded were documented using their respective Julian Day Number and Julian Date. Julian Day numbers record a given date using a continuous increasing integer that started on January 1, 4713 BC; the Julian Date is a more precise number that accounts for the time of day via decimal values (18). For local observations using our telescope, each session was started by slewing to a reference target and calibrating and focusing our telescope. Calibration was performed using the stars Arcturus and Alphecca, which both resided close to 2025ngs and were easily visible. After the telescope was focused, 2025ngs was imaged. Multiple different exposure times were tested to maximize the signal-to-noise ratio while minimizing tracking error. Following this, images of 2025ngs as well as dark images were captured. Dark images were taken either by using an entirely opaque filter or by placing the aperture cover on the telescope. A binning factor of 3x3 or 4x4 was used, depending on how visible 2025ngs was on a given night. Binning sacrificed spatial resolution for higher sensitivity, allowing identification and measurement of the supernova when it was visually dimmer.

Julian Date	T_{gr}	C_{gr}	T_g	C_g
2460865.775	1.476	0.376	0.423	25.598
2460867.775	1.564	0.329	0.361	25.688
2460874.878	1.045	0.560	0.008	26.738
2460879.587	1.187	0.494	-0.110	24.702
2460882.687	1.084	0.496	-0.051	27.126
2460884.617	1.021	0.428	-0.007	24.505
2460886.674	0.737	0.432	-0.058	26.511

Table 3. Least squares regression line coefficients for each supernova measurement. The table shows calculated slopes and y-intercepts to transform between instrumental and standard magnitudes.

Image processing

Raw images were converted to solved Flexible Image Transport System or FITS files by stacking them using the astronomical image processing tool Siril, subtracting the stacked dark image from both the stacked green and red images, and then solving them using field solving software from astrometry.net (19, 20). FITS files are the standard digital file format used in astrophysics to store, archive, and share scientific data. They contain raw, numerical data often in the form of 1D spectra, 2D tables, or 3D data cubes, and can support the World Coordinate Systems, which map pixels to physical sky coordinates. Once the solved FITS files were obtained for both filters, the files were processed using an aperture photometry program we created. In this program, we used the AAVSO APASS DR10 reference data sheet, containing nearby calibration stars' right ascension, declination, and standard Sloan g and r filter magnitudes (21).

Our photometric analysis pipeline, coded in Python, consisted of aperture photometry logic, a least squares regression, and root mean squared uncertainty calculation. The photometry portion of our pipeline was used to calculate the instrumental fluxes and convert them to instrumental magnitudes for both filters, while making use of the Astropy library for converting right ascension and declination into pixel x and y values (22). Along with the standard magnitudes, those values were input into a least squares regression algorithm to generate a best-fit line, yielding the regression coefficients. Of these coefficients, Tgr and Cgr were the slope and intercept of the best-fit line of the equation calculating the color index of 2025ngs, respectively **(Table 3)**. Likewise, Tg and Cg were the slope and intercept of the best-fit line for the equation determining the color offset. These fitting equations are detailed below, in which G (green) and R (red) are the standard g and r magnitudes with G – R being the final color index, g (green) and r (red) are the instrumental g and r magnitudes, and Tgr, Cgr, Tg, and Cg were the transformation coefficients used to fit our data to the light curve:

$$G - R = T_{gr}(g-r) + C_{gr} \quad \text{(Equation 2)}$$

$$G - g = T_{g}(G - R) + C_{g} \quad \text{(Equation 3)}$$

Uncertainty values for each filter were determined by taking the root mean square of the residuals from each best-fit line. The regression coefficients were used to transform the instrumental magnitudes of 2025ngs to standard apparent magnitudes for each filter **(Table 2)**. Finally, the distance to our supernova was calculated using the distance modulus equation: m is the apparent magnitude; M is the standard magnitude; and d is the distance:

$$m - M = 5\text{Log}_{10}(d) - 5 \quad \text{(Equation 1)}$$

ACKNOWLEDGMENTS

We thank all of the faculty, academic or otherwise, at the Yale Summer Program in Astrophysics who assisted us with this project. This includes, but is not limited to, Ms. Emily Sheehan, Ms. Kyra Bettwy, Mr. Ellis Eisenberg, and Ms. Nikki Wu. We would also like to thank our telescope operation staff, Mr. Surendra Bhattarai and Mr. Will Cerny.

Appendix

https://github.com/kellylhaberkorn-ctrl/supernova-photometry-pipeline.

Received: October 8, 2025
Accepted: May 12, 2026
Published: September 4, 2026

REFERENCES

1. "Supernovae." *Sensing the Dynamic Universe – Harvard and Smithsonian Center for Astrophysics*. lweb.cfa.harvard.edu/sdu/supernovae.html. Accessed 17 April 2026.
2. Chandrasekhar, S. "The Maximum Mass of Ideal White Dwarfs." *The Astrophysical Journal*, vol. 74, 1 July 1931, p. 81. https://doi.org/10.1086/143324
3. "Type II Supernova Light Curves." *COSMOS – The SAO Encyclopedia of Astronomy*. https://astronomy.swin.edu.au/cosmos/T/Type+II+Supernova+Light+Curves. Accessed 1 August 2025.
4. González-Bañuelos, M., et al. "Statistical analysis of early spectra in Type II and IIb supernovae." *Astronomy & Astrophysics*, vol. 702, October 2025, https://doi.org/10.1051/0004-6361/202554629
5. Tonry, J., et al. "ATLAS Transient Discovery Report for 2025-06-12." *Transient Name Server Discovery Report*, vol. 2025-2188, 12 June 2025, pp. 1. https://www.wis-tns.org/object/2025ngs/discovery-cert
6. Bostroem, K.A., et al. "DLT40 Transient Classification Report for 2025-06-13." *Transient Name Server Classification Report*, vol 2025-2207, June 2025, thttps://www.wis-tns.org/object/2025ngs/classification-cert
7. Zaninetti, L., "Sparse Formulae for the Distance Modulus in Cosmology." *Journal of High Energy Physics, Gravitation and Cosmology*, vol. 07, no. 3, 10 July 2021, pp. 965–992. https://doi.org/10.4236/jhepgc.2021.73057
8. Dessart, L., et al. "Type II-Plateau supernova radiation: dependences on progenitor and explosion properties." *Monthly Notices of the Royal Astronomical Society*, vol. 433, no. 2, 1 Aug 2013, pp. 1745–1763. https://doi.org/10.1093/mnras/stt861
9. Chieffi, A., et al. "Theoretical light curves of Type II-P supernovae and applications to cosmology." *Monthly Notices of the Royal Astronomical Society*, vol. 345, no 1, Oct 2003, pp. 111–122. https://doi.org/10.1046/j.1365-8711.2003.06958.x
10. Takáts, K., et al. "SN 2009ib: a Type II-P supernova with an unusually long plateau." *Monthly Notices of the Royal Astronomical Society,* vol. 450, no 3, 1 July 2015, pp. 3137–3154, https://doi.org/10.1093/mnras/stv857
11. Yang, S., et al. "A low-energy explosion yields the underluminous Type IIP SN 2020cxd." *Astronomy & Astrophysics,* vol 655, no. A90, 25 Nov 2021, pp. 1–19. https://doi.org/10.1051/0004-6361/202141244
12. Bartunov, O., et al. "A comparative study of type I and type II supernovae." *Astrophysics and Space Science,* vol. 122, May 1986, pp. 343-354. https://doi.org/10.1007/BF00650200
13. Li, W., et al. "Nearby Supernova Rates from the Lick Observatory Supernova Search - II. The Observed Luminosity Functions and Fractions of Supernovae in a Complete Sample." *Monthly Notices of the Royal Astronomical Society*, vol. 395, no. 3, 8 May 2009, pp. 1409–1437, https://doi.org/10.1111/j.1365-2966.2009.14506.x
14. Karachentsev, I.D., et al. "Nearby groups of galaxies in the Hercules–Bootes constellations." *Astrophysical Bulletin,* vol. 72, 27 May 2017, pp. 111–121. https://doi.org/10.1134/S1990341317020031
15. Mitchell, R.C., et al. "Locating Type II-P Supernovae Using the Expanding Photosphere Method. I. Comparing Distances from Different Line Velocities." *The Astrophysical Journal,* vol. 942, no. 1, 6 Jan 2023, p. 38. https://doi.org/ 10.3847/1538-4357/aca415
16. De Jaeger, T., et al. "Observed Type II supernova colours from the Carnegie Supernova Project-I." *Monthly Notices of the Royal Astronomical Society*, vol. 476, no. 4, 24 February 2018, pp. 4592–4616, https://doi.org/10.1093/mnras/sty508
17. Barthelmy, S.D., et al. "GRB Coordinates Network (GCN): A Status Report." *Gamma-Ray Bursts, 5th Huntsville Symposium*, vol. 526, 8 Sep 2000, pp. 731–735. https://doi.org/10.1063/1.1361631.
18. McCarthy, Dennis. "The Julian and Modified Julian Dates." Journal for the History of Astronomy, vol. 29, 1998, pp.

327–330, https://doi.org/10.1177/002182869802900402.
19. Richard, C., et al. "Siril: An Advanced Tool for Astronomical Image Processing." *Journal of Open Source Software*, vol. 9, no. 102, 1 Aug 2024, https://doi.org/10.21105/joss.07242
20. Lang, D., et al. "Astrometry.net: Blind astrometric calibration of arbitrary astronomical images." *The Astronomical Journal*, vol. 139, no. 5, 22 Mar 2010, https://doi.org/10.1088/0004-6256/139/5/1782.
21. Henden, A., et al. "APASS Data Release 10." *American Astronomical Society Meeting Abstracts*, vol. 232, June 2018, pp. 223. https://ui.adsabs.harvard.edu/abs/2018AAS...23222306H/abstract.
22. Price-Whelan, A., et al. "The Astropy Project." arXiv, 2022, https://arxiv.org/abs/2206.14220

Copyright: © 2026 Bavas, Gerstein, Haberkorn, Garrett, Warrener, and Faison. All JEI articles are distributed under the Creative Commons Attribution Noncommercial No Derivatives 4.0 International License. This means that you are free to share, copy, redistribute, remix, transform, or build upon the material for any purpose, provided that you credit the original author and source, include a link to the license, indicate any changes that were made, and make no representation that JEI or the original author(s) endorse you or your use of the work. The full details of the license are available at https://creativecommons.org/licenses/by-nc-nd/4.0/deed.en.